Supplementary Information

Syntheses of Sandwich-like $Co_{15}Fe_{85}$@C/RGO Multicomponent Composites with Tunable Electromagnetic Parameters and Microwave Absorption Performance

Susu Bao, Wen Tang, Zhijia Song, Qiaorong Jiang, Zhiyuan Jiang and Zhaoxiong Xie*

State Key Laboratory of Physical Chemistry of Solid Surfaces, and College of Chemistry and Chemical Engineering, Xiamen University, Xiamen 361005, China.

* Corresponding Author: E-mail: zyjiang@xmu.edu.cn (Z. Y. Jiang)

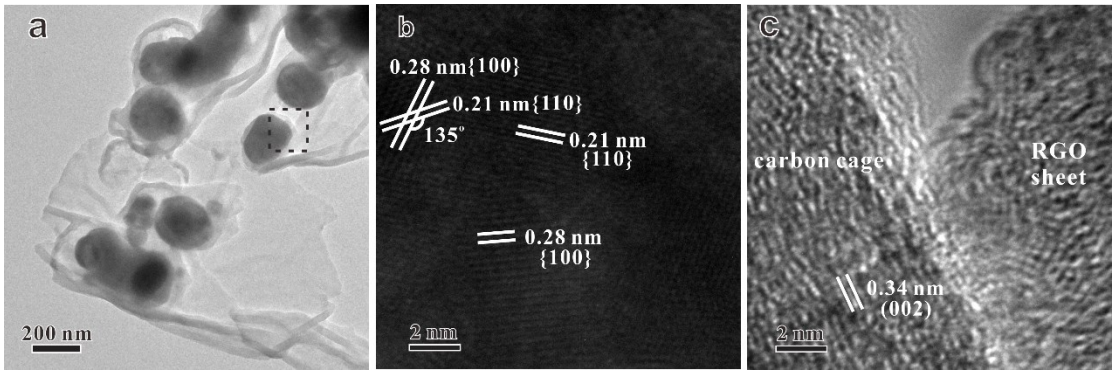

Figure S1. (a) TEM image of $Co_{15}Fe_{85}$@C/RGO-2; (b) HRTEM image of metal alloy cores; and (c) HRTEM image of carbon cage and RGO sheet obtained in the area marked in (a).

Because the atomic numbers of Fe and Co are much larger than that of C, the cores of $Co_{15}Fe_{85}$@C/RGO can be easily identified by the contrast in TEM images (Figure S1a). The fringes spacing of 0.20 and 0.28 nm in the core agree with the {110} and {100} lattice planes of $Co_{15}Fe_{85}$ alloy (Figure S1b). The obvious disorientation of the fringes can be observed, indicating that the alloy cores are polycrystalline. Only a few lattice fringes corresponding to (002) plane of graphite carbon can be observed in the carbon cage (Figure S1c), indicating that the shells are amorphous or low graphitic carbon.

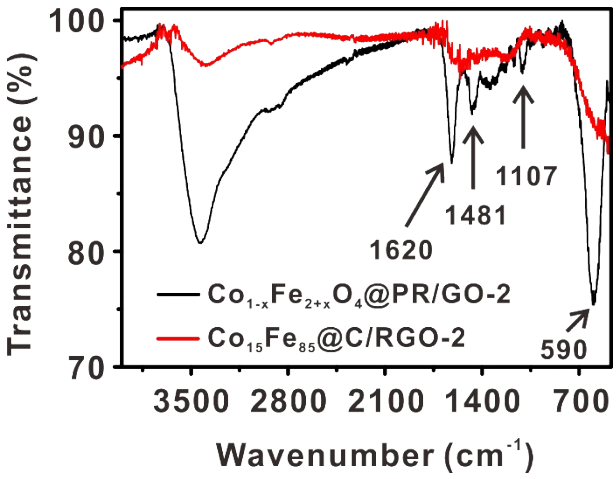

Figure S2. FT-IR spectra of $Co_{1-x}Fe_{2+x}O_4$@PR/GO-2 and $Co_{15}Fe_{85}$@C/RGO-2.

Both samples show broad peak around 3400 cm^{-1} (O−H stretching band), the strength of $Co_{15}Fe_{85}$@C/RGO-2 is obviously weakened, indicating that the hydroxyl group of $Co_{1-x}Fe_{2+x}O_4$@PR/GO-2 is greatly reduced after calcination. $Co_{1-x}Fe_{2+x}O_4$@PR/GO-2 has characteristic spectral signal of phenolic resin, such as C=C aromatic ring stretching at 1620 cm^{-1}, methylene bridge C−H bend at 1481 cm^{-1} and methylene-ether bridge C−O−C bend at 1107 cm^{-1}, which have not been found for $Co_{15}Fe_{85}$@C/RGO-2, indicating that the phenolic resin has been transformed into C. The band around 590 cm^{-1} shows the stretching vibrations of tetrahedral Fe−O, which can be seen obviously at IR spectra of $Co_{1-x}Fe_{2+x}O_4$@PR/GO-2, but disappears at the spectra of $Co_{15}Fe_{85}$@C/RGO-2, which is consistent with the reduction process of $Co_{1-x}Fe_{2+x}O_4$ to CoFe alloy.

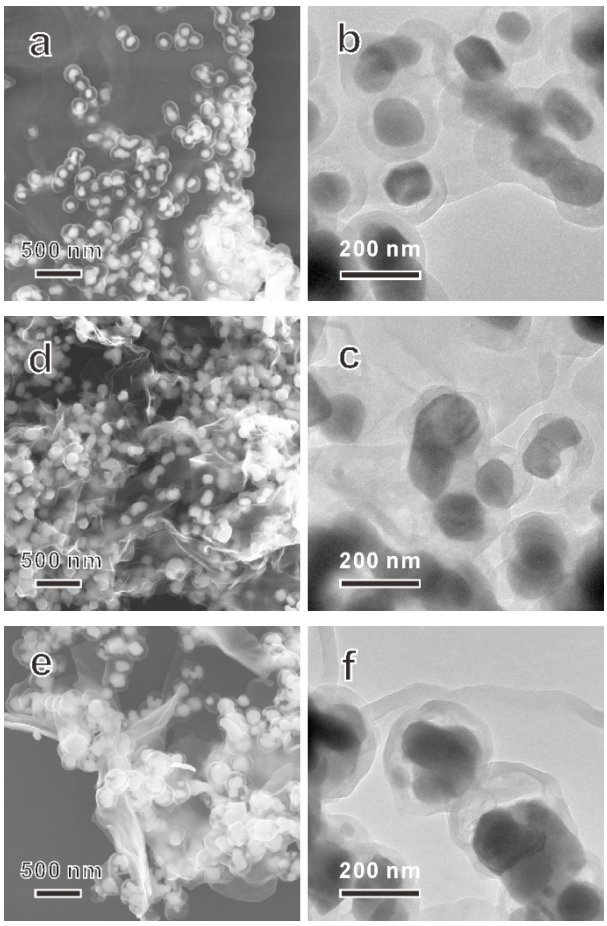

Figure S3. Structural features of $Co_{15}Fe_{85}$@C/RGO sandwich structures. (a) SEM image and (b) TEM image of $Co_{15}Fe_{85}$@C/RGO-1, (c) SEM image and (d)TEM image of $Co_{15}Fe_{85}$@C/RGO-3, (e) SEM image and (f) TEM image of $Co_{15}Fe_{85}$@C/RGO-4.

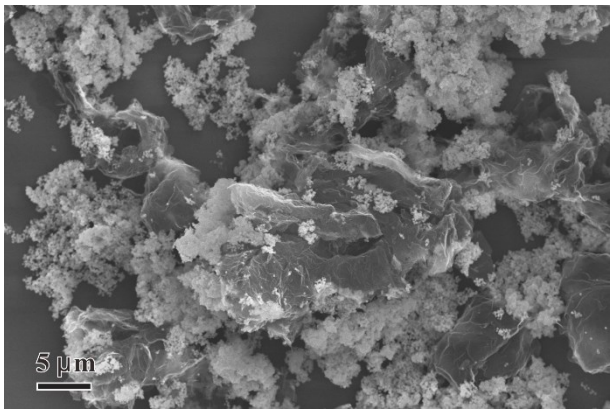

Figure S4. Typical SEM image of the products obtained by using grephene sheets directly in the synthesis process. Instead of sandwich structures, the magnetic particles tend to agglomerate together and only loosely mix with graphene sheets.

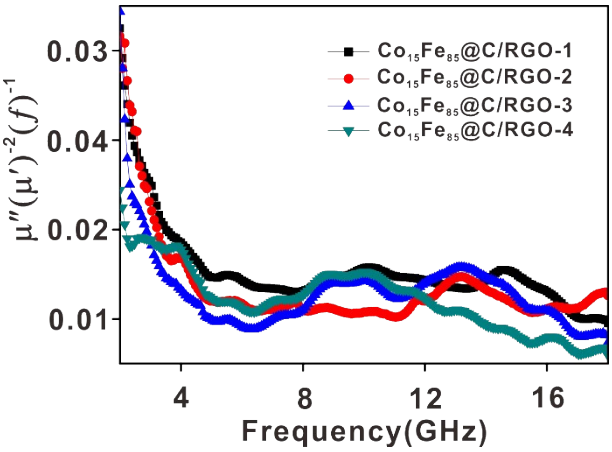

Figure S5. Frequency dependence of $\mu''(\mu')^{-2}(f)^{-1}$ of $Co_{15}Fe_{85}$@C/RGO-1, $Co_{15}Fe_{85}$@C/RGO-2, $Co_{15}Fe_{85}$@C/RGO-3 and $Co_{15}Fe_{85}$@C/RGO-4, respectively.

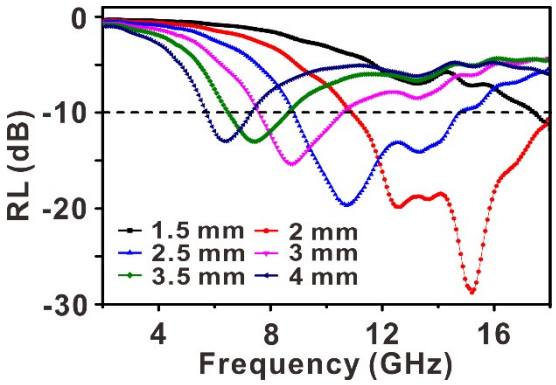

Figure S6. The calculated RL of the product obtained by using grephene sheets instead of GO in the synthesis process. The sample contains 60 wt % of the as-prepared products and 40 wt% paraffin. With a thickness of 2.0 mm, the strongest RL is up to -28.8 dB at 15.2 GHz, and the effective absorption bandwidth is 7.2 GHz.

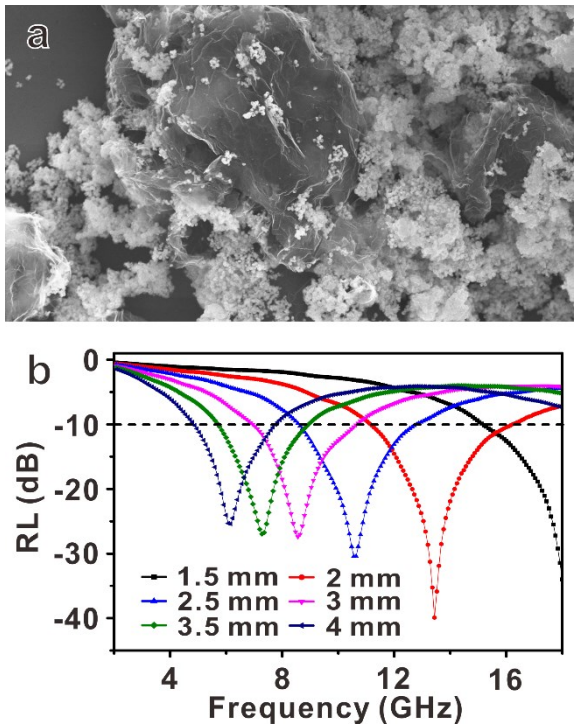

Figure S7. (a) Typical SEM image of the product obtained by physical mixing of $Co_{15}Fe_{85}$@C and RGO with the same ratio of the $Co_{15}Fe_{85}$@C/RGO-2 sample, (b) The calculated reflection loss of the above physical mixed samples (60 wt %) with paraffin.

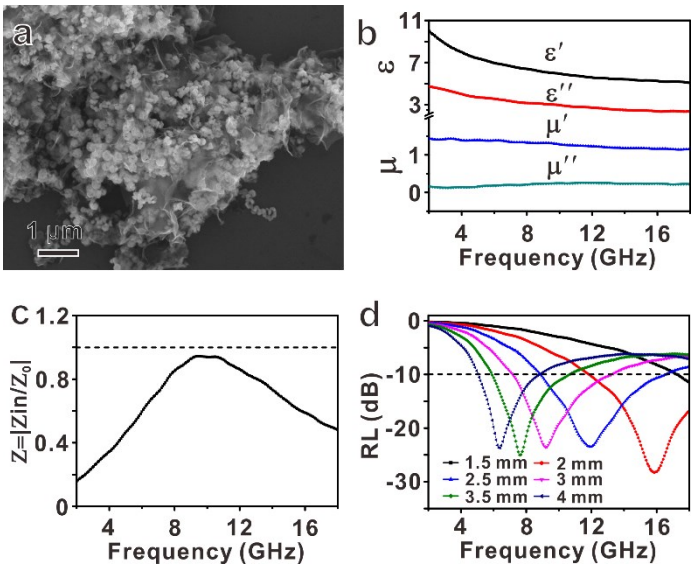

Figure S8. (a) SEM image of $Co_{15}Fe_{85}$@C/RGO with smaller void space (The feed ratio of the sample is the same as $Co_{15}Fe_{85}$@C/RGO-2), (b) the electromagnetic properties, (c) the coefficient of electromagnetic matching with a thickness of 2.5 mm, and (d) the calculated reflection loss (RL) of the sample with given thickness.

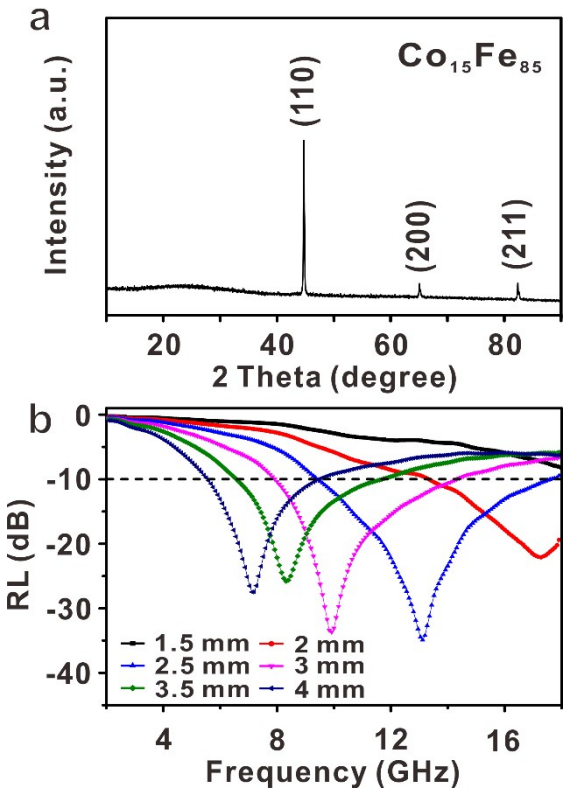

Figure S9. (a) XRD pattern and (b) the calculated reflection loss curves of $Co_{15}Fe_{85}$@C/RGO-2 kept in ambient atmosphere at room temperature for 6 months. With a thickness of 2.5 mm, the strongest RL is up to -34.9 dB at 13.12 GHz, and the effective absorption bandwidth is 8.3 GHz.

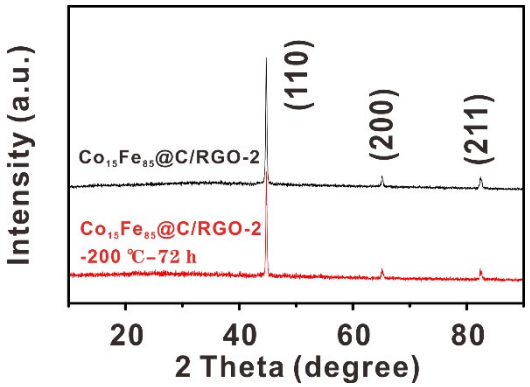

Figure S10. XRD pattern of $Co_{15}Fe_{85}$@C/RGO-2 before (black) and after (red) heating in the air at 200 °C for 72 h.

Table S1. Atomic ratio and metal content of the $Co_{15}Fe_{85}$@C/RGO sandwich structure determined by ICP-OES

Samples	n_{Fe}/n_{Co}	metal content (%)
$Co_{15}Fe_{85}$@C/RGO-1	5.3	78 ± 2
$Co_{15}Fe_{85}$@C/RGO-2	5.5	77 ± 2
$Co_{15}Fe_{85}$@C/RGO-3	5.6	74 ± 2
$Co_{15}Fe_{85}$@C/RGO-4	5.4	73 ± 2

Table S2. Carbon contents of different $Co_{15}Fe_{85}$@C/RGO composites measured by elementary analysis method

Samples	The mass percent of carbon (wt %)	Calcination temperature (ºC)
$Co_{15}Fe_{85}$@C/RGO-1	19.8 ± 0.5	500
$Co_{15}Fe_{85}$@C/RGO-2	21.2 ± 0.5	500
$Co_{15}Fe_{85}$@C/RGO-3	25.3 ± 0.5	500
$Co_{15}Fe_{85}$@C/RGO-4	28.1 ± 0.5	500